

Article

Short I ··· O Interactions in the Crystal Structures of Two 2-Iodo-Phenyl Methyl-Amides as Substrates for Radical Translocation Reactions

 Ahtsham Ishaq, John M. D. Storey and William T. A. Harrison * 

Department of Chemistry, University of Aberdeen, Meston Walk, Aberdeen AB24 3UE, Scotland, UK; a.ishaq@abdn.ac.uk (A.I.); j.storey@abdn.ac.uk (J.M.D.S.)

* Correspondence: w.harrison@abdn.ac.uk; Tel.: +44-(0)1224-272897

Abstract: Radical translocation reactions are finding various uses in organic synthesis, in particular the stereospecific formation of complex natural products. In this work, the syntheses and single-crystal structures of two substituted 2-iodo-phenyl methyl-amides are reported, namely *cyclo*-propane carboxylic acid (2-iodo-phenyl)-methyl-amide, C₁₁H₁₂INO (1), and *cyclo*-heptane carboxylic acid (2-iodo-phenyl)-methyl-amide, C₁₅H₂₀INO (2). In each case, the methyl-amide group has a *syn* conformation, and this grouping is perpendicular to the plane of the benzene ring: these solid-state conformations appear to be well setup to allow an intramolecular hydrogen atom transfer to take place as part of a radical translocation reaction. Short intermolecular I ··· O halogen bonds occur in each crystal structure, leading to [010] chains in 1 [I ··· O = 3.012 (2) Å] and isolated dimers in 2 [I ··· O = 3.024 (4) and 3.057 (4) Å]. The intermolecular interactions are further quantified by Hirshfeld surface analyses.

Keywords: methyl-amides; halogen bonds; conformational analysis



Citation: Ishaq, A.; Storey, J.M.D.; Harrison, W.T.A. Short I ··· O Interactions in the Crystal Structures of Two 2-Iodo-Phenyl Methyl-Amides as Substrates for Radical Translocation Reactions. *Chemistry* **2023**, *5*, 1233–1242. <https://doi.org/10.3390/chemistry5020083>

Academic Editor: Katharina M. Fromm

Received: 11 April 2023

Revised: 2 May 2023

Accepted: 3 May 2023

Published: 12 May 2023



Copyright: © 2023 by the authors. Licensee MDPI, Basel, Switzerland. This article is an open access article distributed under the terms and conditions of the Creative Commons Attribution (CC BY) license (<https://creativecommons.org/licenses/by/4.0/>).

1. Introduction

Radical translocation reactions (radical generation by photolysis, heat, or reaction with an initiator, followed by an intramolecular H atom shift) have found various uses in organic synthesis, from forming simple carbocycles [1] to complex natural products [2,3]. These reactions rely on the translocation (i.e., H atom migration) of an initially generated radical to a remote site, usually four [4] to seven [5] atoms away. Figure 1 illustrates the general principle involved.

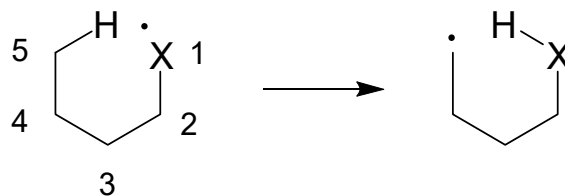


Figure 1. Schematic of a 1,5-hydrogen atom abstraction reaction (X = C, N or O).

The driving force behind the rearrangement is assumed to be the formation of a more stable radical after translocation; typically, the initially formed radical is an aryl or vinyl species, perhaps formed by photolytic cleavage of a C—X (X = halogen) bond in a benzene ring, which is unstable and highly reactive [6]. The high reactivity and lack of stability of these radicals is presumed to be a result of the lone electron occupying an σ -orbital that is orientated perpendicular to the aromatic/conjugated π system, and therefore, stabilization of the radical by delocalization is not possible.

In order for the intramolecular translocation reaction to occur, it has been determined that the molecule must adopt a *cis* conformation [7], in which the two components (the initial radical and the C—H bond to supply the transferrable H atom) face each other, and the use of a suitable *N*-bonded substituent attached to the aromatic ring can provide a ‘conformational lock’, thereby optimizing the likelihood of translocation and subsequent cyclization [8]. In order to help further understand this process, the related compounds *cyclo*-propane carboxylic acid (2-iodo-phenyl)-methyl-amide (alternative name: *N*-(2-iodophenyl)-*N*-methylcyclopropanecarboxamide), C₁₁H₁₂INO (**1**), and *cyclo*-heptane carboxylic acid (2-iodo-phenyl)-methyl-amide (alternative name: *N*-(2-iodophenyl)-*N*-methylcycloheptanecarboxamide), C₁₅H₂₀INO (**2**), were prepared, and their crystal structures were determined.

2. Materials and Methods

2.1. Synthesis of **1**

Cyclopropane carbonyl chloride (1.04 g, 10.4 mmol) was added dropwise to a solution of 2-iodoaniline (2.00 g, 9.13 mmol) and *N,N*-diisopropylethylamine (Hünig’s base or DIPEA) (1.53 g, 11.9 mmol) in tetrahydrofuran (THF) (20 mL) at 0 °C under nitrogen (Figure 2). The solution was then allowed to warm to room temperature and stirring was continued for a further four hours. The reaction mixture was then diluted with diethyl ether (50 mL) and washed with brine (2 × 30 mL) and then water (30 mL). The ether layer was then dried with MgSO₄ and filtered, and the solvent was removed at reduced pressure. The product was purified by recrystallization from the mixed solvents of dichloromethane and hexane, yielding cyclopropane carboxylic acid (2-iodo-phenyl)-amide (**3**) (Figure 1) as a white solid (2.49 g, 95%); m.p. 111–113 °C; HRMS: found MH⁺, 287.9885, C₁₀H₁₁INO requires M⁺ 287.9885; $\nu(\text{KBr}/\text{cm}^{-1})$ 3280, 2998, 1667, 1480, 1456, 1393, 1241; ¹H NMR δ_{H} (250 MHz, CDCl₃) 1.65 (2H, m, CH₂), 1.79 (2H, m, CH₂), 2.79 (1H, m, CH), 6.82 (1H, dd apparent t, *J* 7.3, 7.9, ArH-4), 7.33 (1H, dd apparent t, *J* 7.6, 7.9, ArH-5), (7.48 (1H, br s, NH), 7.76 (1H, d, *J* 7.3, ArH-3), 8.25 (1H, d, *J* 7.6, ArH-6); ¹³C NMR δ_{C} (62.5 MHz, CDCl₃) 26.0 (CH₂), 30.5 (CH₂), 47.2 (CH), 99.8 (quaternary ArC), 121.8 (Ar-CH), 125.7 (Ar-CH), 129.3 (Ar-CH), 138.3 (quaternary ArC), 138.7 (Ar-CH) 174.5 (C=O).

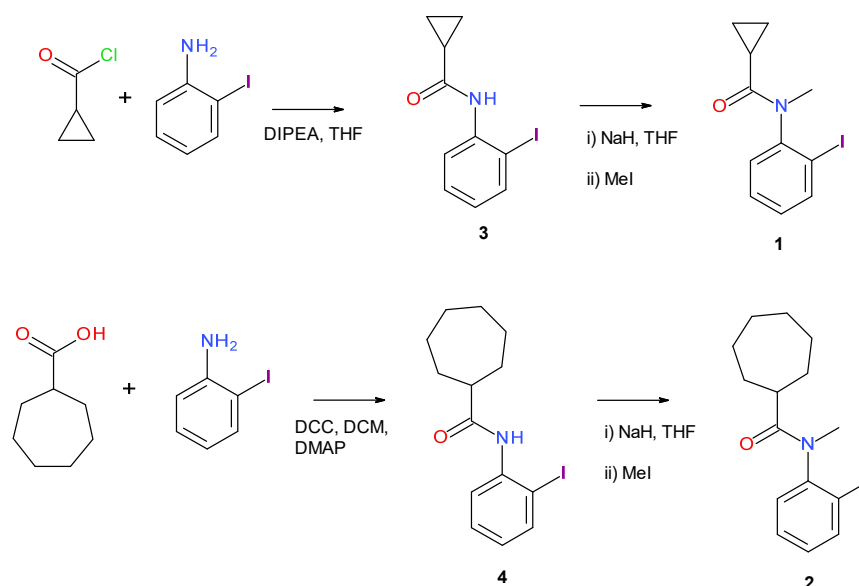


Figure 2. Synthesis schemes for **1** and **2** via intermediates **3** and **4** (see the text for abbreviations).

A solution of **3** (1.00 g, 3.48 mmol) in THF (10 mL) was added dropwise to a suspension of sodium hydride (502 mg, 4.53 mmol) in dry THF (20 mL) at 0 °C. Once hydrogen evolution had ceased, iodomethane (497 mg, 3.48 mmol) was added to the solution and was allowed to stir overnight. The reaction was quenched with ammonium chloride solution

(2 mL) and diluted with diethyl ether (50 mL). The ethereal solution was washed with brine (2 × 30 mL) and then water (30 mL). The ethereal solution was then dried with MgSO₄, filtered, and solvent was removed at reduced pressure. The crude product was purified by column chromatography, eluting with hexane/ethyl acetate (4:1), yielding **1** as a colorless solid (942 mg, 90%); m.p. 97–99 °C; HRMS: found MH⁺, 302.0032 C₁₁H₁₂INO requires MH⁺ 302.0036; ν (KBr/cm⁻¹) 2970, 1667, 1467, 1425, 1388, 1281; δ _H (250 MHz, CDCl₃) 1.57 (2H, m, CH₂), 1.85 (2H, m, CH₂), 1.03 (1H, m, CH), 3.06 (3H, s, NCH₃), 7.01 (1H, dd (apparent t), *J* 7.9, 7.4, ArH-5), 7.22 (1H, d, *J* 7.7, ArH-3), 7.42 (1H, dd apparent t, *J* 7.7, 7.4, ArH-4), 7.90 (1H, d, *J* 7.9, ArH-6); δ _C (62.5 MHz, CDCl₃) 8.2 (CH₂), 8.9 (CH₂), 12.6 (CH), 36.2 (NCH₃), 100.0 (quaternary ArC), 129.4 (Ar-CH), 129.7 (Ar-CH), 129.8 (Ar-CH), 140.1 (Ar-CH), 146.4 (quaternary ArC), 173.4 (C=O). Colorless crystals of **1** were grown by recrystallization from ethyl acetate solution.

2.2. Synthesis of **2**

The 2-iodoaniline (3.00 g, 13.7 mmol) was added to a solution of cycloheptane carboxylic acid (2.4 g, 17 mmol) in dichloromethane (DCM) (20 mL). A solution of di-cyclohexylcarbodiimide (DCC) (3.17 g, 15.4 mmol) in DCM (10 mL) was then added dropwise at 0 °C and 4-(dimethylamino)pyridine (DMAP) (0.17 g, 0.14 mmol) was added as a catalyst. The resulting solution was stirred for 30 min at room temperature then cooled in ice, and the solid was filtered off and washed with DCM. The filtrate was collected and washed with 2 N HCl solution (3 × 30 mL), and then with saturated NaHCO₃ solution (3 × 30 mL) and water (30 mL). The organic layer was collected and dried over MgSO₄, filtered, and the solvent was removed at reduced pressure. The crude product was then purified by column chromatography, eluting with hexane/ethyl acetate (3:1), yielding cycloheptane-carboxylic acid (2-iodo-phenyl)-amide (**4**) as a white solid (2.97 g, 63%); m.p. 136–138 °C; HRMS: found MH⁺, 344.0506 C₁₄H₁₉INO requires M⁺ 344.0506; ν (neat/cm⁻¹) 2965, 2905, 1672, 1481, 1411, 1351; ¹H NMR δ _H (250 MHz, CDCl₃) 1.52–1.65 (6H, m, cycloheptane CH₂), 1.71–1.88 (4H, m, cycloheptane CH₂), 1.99–2.14 (2H, m, cycloheptane, CH₂), 2.39 (1H, m, CH), 6.84 (1H, dd (apparent t), *J* 6.9, 7.6, ArH-5) 7.33 (1H, dd apparent t, *J* 7.6, 7.6, Ar-H-4), 7.43 (1H, br s, NH), 7.75 (1H, d, *J* 6.9, ArH-3), 8.24 (1H, d, *J* 7.6, ArH-6); ¹³C NMR δ _C (62.5 MHz, CDCl₃) 26.5 (2 × CH₂), 28.3 (2 × CH₂), 31.7 (2 × CH₂), 48.6 (CH), 99.8 (quaternary ArC), 121.9 (Ar-CH), 125.7 (Ar-CH), 129.3 (Ar-CH), 138.2 (quaternary ArC), 138.7 (Ar-CH), 175.5 (C=O).

A solution of **4** (500 mg, 1.45 mmol) in dry THF (5 mL) was added dropwise to a suspension of sodium hydride (45 mg, 1.89 mmol) in dry THF (10 mL) at 0 °C. Once hydrogen evolution had ceased, iodomethane (227 mg, 1.60 mmol) was added and the solution was allowed to stir overnight. The reaction was quenched with ammonium chloride solution (2 mL) and taken up in diethyl ether (50 mL). The ethereal solution was washed with brine (2 × 30 mL) and water (30 mL). The ethereal solution was then dried over MgSO₄, filtered, and then reduced to yield the crude product, which was purified by column chromatography, eluting with hexane/ethyl acetate (3:1), yielding **2** as a white solid (454 mg, 88%); m.p. 119–121 °C; HRMS: found MH⁺, 358.0670, C₁₅H₂₁INO requires M⁺ 358.0662; ν (KBr/cm⁻¹) 2967, 2884, 1671, 1494, 1408, 1393, 1251; ¹H NMR δ _H (250 MHz, CDCl₃) 0.99–1.08 (1H, m, CH₂), 1.21–1.46 (4H, m, CH₂), 1.51–1.69 (4H, m, CH₂), 1.71–1.80 (2H, m, CH₂), 1.81–1.94 (1H, m, CH₂), 1.99–2.08 (1H, m, CH), 3.14 (3H, s, NCH₃), 7.07 (1H, dd apparent t, *J* 7.6, 7.7, ArH-5), 7.24 (1H, d, *J* 7.3, ArH-3), 7.42 (1H, dd apparent t, *J* 7.3, 7.6, ArH-4), 7.94 (1H, d, *J* 7.7, ArH-6); ¹³C NMR δ _C (62.5 MHz, CDCl₃) 26.6 (CH₂), 26.7 (CH₂), 28.0 (CH₂), 28.3 (CH₂), 31.1, (CH₂) 31.7 (CH₂), 35.9 (CH), 43.2 (NCH₃), 96.1 (quaternary ArC), 128.9 (Ar-CH), 129.6 (Ar-CH), 129.8 (Ar-CH), 140.2 (Ar-CH), 146.4 (quaternary ArC), 177.5 (C=O). Yellow blocks of **2** were grown from ethyl acetate solution.

2.3. X-ray Data Collection and Refinement

The intensity data for **1** were collected on a Bruker SMART1000 CCD diffractometer at 293 K, and the corresponding data for **2** were collected on an Enraf-Nonius KappaCCD

diffractometer at 120 K. Empirical (SADABS multi-scan) absorption corrections were applied at the data reduction stage and the structures were routinely solved by direct methods with SHELXS-97, while the atomic models were completed and optimized by refinement against $|F|^2$ with SHELXL-2018. One of the *cyclo*-heptyl rings in **2** is disordered over two orientations for atoms C26, C28, and C29 and their attached H atoms in a 0.60 (3):0.40 (3) ratio. The H atoms were mostly located in difference maps and relocated to idealized locations (C—H = 0.93–0.97 Å), and they were further refined as riding atoms with the constraint $U_{\text{iso}}(\text{H}) = 1.2U_{\text{eq}}(\text{C})$ or $1.5U_{\text{eq}}(\text{methyl C})$ applied. The methyl groups were allowed to rotate, but not to tip, to best fit the electron density. Full details are provided in the deposited cifs.

Crystal data for **1**: colorless blade, $0.40 \times 0.15 \times 0.05$ mm, $\text{C}_{11}\text{H}_{12}\text{INO}$, $M_r = 301.12$, monoclinic, $P2_1$ (No. 4), $a = 9.1609$ (5) Å, $b = 6.7614$ (4) Å, $c = 9.8332$ (5) Å, $\beta = 109.473$ (1)°, $V = 574.23$ (5) Å³, $Z = 2$, $T = 293$ K, Mo K α radiation, $\lambda = 0.71073$ Å, $\rho_{\text{calc}} = 1.742$ g cm⁻³, $\mu = 2.757$ mm⁻¹, 6836 reflections measured ($-13 \leq h \leq 13$, $-8 \leq k \leq 10$, $-14 \leq l \leq 14$; $4.4^\circ \leq 2\theta \leq 65.0^\circ$), $R_{\text{Int}} = 0.015$, 3296 merged reflections, Flack absolute structure parameter = 0.56 (2), $R(F)$ (2726 reflections with $I > 2\sigma(I)$) = 0.026, $wR(F^2)$ (all data) = 0.062, min./max. $\Delta\rho = -0.32, +0.97 e \text{ \AA}^{-3}$. CSD deposition number: 2254542.

Crystal data for **2**: yellow cuboid, $0.20 \times 0.20 \times 0.20$ mm, $\text{C}_{15}\text{H}_{14}\text{INO}$, $M_r = 357.22$, orthorhombic, $P2_12_12_1$ (No. 19), $a = 8.8958$ (2) Å, $b = 13.8911$ (5) Å, $c = 24.3439$ (7) Å, $V = 3038.67$ (16) Å³, $Z = 8$, $T = 120$ K, Mo K α radiation, $\lambda = 0.71073$ Å, $\rho_{\text{calc}} = 1.562$ g cm⁻³, $\mu = 2.098$ mm⁻¹, $T_{\text{min}} = 0.679$, $T_{\text{max}} = 0.679$, 21,877 reflections measured ($-10 \leq h \leq 11$, $-18 \leq k \leq 15$, $-31 \leq l \leq 31$; $6.4^\circ \leq 2\theta \leq 55.0^\circ$), $R_{\text{Int}} = 0.041$, 6845 merged reflections, Flack absolute structure parameter = 0.09 (3), $R(F)$ (6163 reflections with $I > 2\sigma(I)$) = 0.040, $wR(F^2)$ (all data) = 0.103, min./max. $\Delta\rho = -0.81, +2.55 e \text{ \AA}^{-3}$. CSD deposition number: 2254543.

3. Results and Discussion

3.1. Structure of $\text{C}_{11}\text{H}_{12}\text{INO}$ (**1**)

Compound **1** crystallizes in the monoclinic space group $P2_1$ with one molecule in the asymmetric unit (Figure 3). The dihedral angle between the mean planes of the C1–C6 benzene ring and the C7/C8/N1/O1 methyl-amide grouping is 86.09 (14)°. The bond-angle sum at N1 of 360.0° implies the expected sp^2 hybridization for this atom, and its un-hybridized $2p$ orbital is therefore well-aligned to interact with the π system of the adjacent C=O group, as reflected in the typical amide C8–N1 bond length of 1.357 (4) Å. However, this $2p$ orbital lies almost perpendicular to the delocalized π system of the benzene ring, and therefore, the C6–N1 bond length of 1.435 (4) Å is essentially that of a single bond. The conformation of the methyl-amide group is *syn* (C7–N1–C8–O1 torsion angle = 2.5 (5)°), as is the conformation of the C6–N1–C8–C9 grouping (2.6 (5)°). The dihedral angle between the C7/C8/N1/O1 grouping and the C9/C10/C11 *cyclo*-propyl ring is 86.3 (3)°, and the dihedral angle between the benzene and *cyclo*-propyl rings is 58.7 (3)°. The *cyclo*-propyl ring is, of course, strictly planar, and the terminal C10–C11 bond length of 1.471 (6) Å is notably shorter than the other two bonds (1.500 (5) and 1.502 (5) Å), which is normal when an unsaturated substituent is attached to the methine group [9]. The C10–C9–C11 bond angle of 58.7 (3)° is notably smaller than the C9–C10–C11 and C9–C11–C10 angles (60.7 (3) and 60.6 (3)°, respectively). The overall conformation of the molecule of **1** could be described as V-shaped, in which the C9–H9 bond (i.e., the methine group of the *cyclo*-propyl ring) faces the C1–I1 bond in the aromatic ring ($\text{H9}\cdots\text{C1} = 2.94$ Å, $\text{C9–H9}\cdots\text{C1} = 113^\circ$), in what appears to be a very favorable orientation for a 1,5-translocation reaction to occur, assuming that the solid-state conformation is maintained in solution. Key geometrical data for **1** are summarized in Table 1.

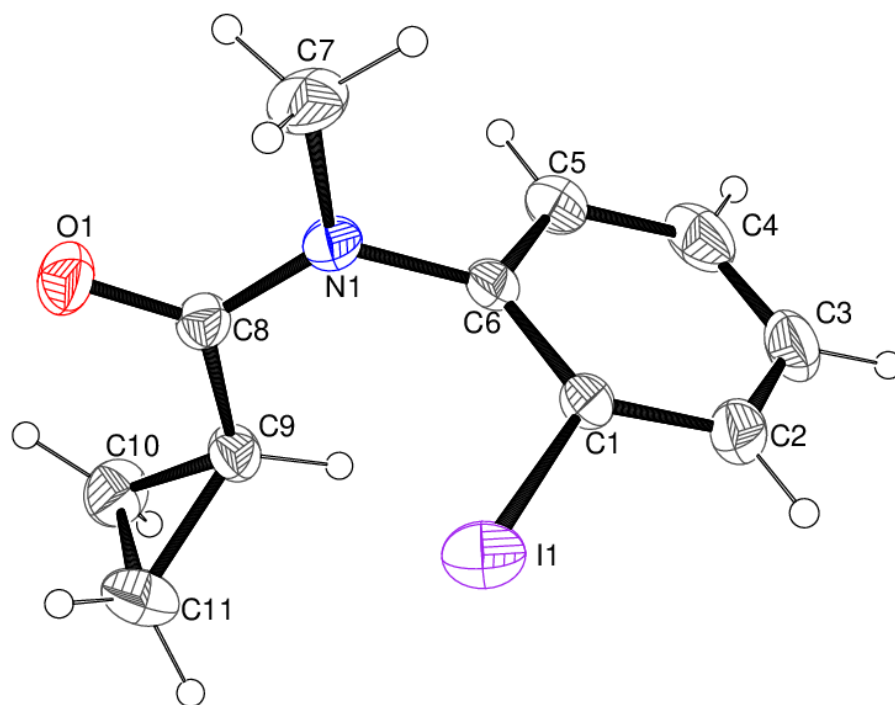


Figure 3. The molecular structure of **1**, showing 50% displacement ellipsoids for the non-hydrogen atoms. Note that the C9—H9 bond faces atom C1 in a favorable orientation for a translocation reaction to occur.

Table 1. Selected geometrical data for molecules **1**, **2A**, and **2B** (Å, °).

	1	2A	2B
C1—I1	2.112 (4)	2.101 (7)	2.096 (7)
C6—N1	1.435 (4)	1.428 (9)	1.431 (10)
C8—N1	1.357 (4)	1.359 (10)	1.370 (9)
C8—O1	1.226 (4)	1.213 (9)	1.236 (8)
C8—C9	1.479 (5)	1.527 (10)	1.533 (10)
O1—C8—N1	121.1 (3)	121.8 (7)	120.6 (7)
C6—N1—C8	124.0 (3)	124.3 (6)	123.5 (6)
C6—N1—C7	117.3 (3)	115.4 (6)	117.0 (6)
C7—N1—C8	118.7 (3)	120.3 (6)	119.5 (6)
C1—C6—N1—C8 (φ)	−87.2 (4)	−89.5 (7)	−90.3 (7)
C7—N1—C8—O1 (ξ)	2.5 (5)	0.8 (8)	2.9 (7)
C6—N1—C8—C9 (ψ)	2.6 (5)	−0.2 (7)	0.4 (7)
I···O	3.012 (2)	3.024 (4)	3.057 (4)
C—I···O	171.78 (9)	171.71 (17)	175.98 (16)
I···O=C	135.3 (2)	114.3 (3)	113.1 (3)
C—I···O=C	−7.8 (4)	−118.4 (7)	−165.5 (7)
I···O=C—N	−87.6 (4)	−82.3 (7)	−85.2 (7)

For molecule **2B**, see Figure 5 for the equivalent atom designations. See the text for further discussion of the torsion angles φ , ξ , and ψ . The acceptor O and C atoms in **1** are generated by the symmetry operation $1-x, y-\frac{1}{2}, -z$.

In the crystal of **1**, a very short C1—I1···O1ⁱ ($i = 1-x, y-\frac{1}{2}, -z$) contact or ‘halogen bond’ [10] with an I···O separation of 3.012 (2) Å occurs, which is some 0.49 Å shorter than the expected Bondi [11] van der Waals’ separation of about 3.50 Å for these two atoms. One way to interpret this directional contact is in terms of an electrostatic attraction between the Lewis base (the lone pair bearing an O atom of the carbonyl group) and an ‘ σ hole’ [12] on the Lewis acid (the iodine atom), which has close parallels with the way that hydrogen bonds can be envisaged [13]. The C—I···O grouping is almost linear (bond angle = 171.78 (9)°), which is quite typical for this type of interaction, and the I···O=C bond angle is 135.3 (2)°.

This I⋯O halogen bond leads to C(6) chains [14] of molecules propagating in the [010] direction in the crystal of **1** (Figure 4), with adjacent molecules related by the operation of the 2_1 screw axis. There are no π - π stacking interactions in **1**, with the shortest separation between the benzene-ring-centroids of nearby molecules in the crystal being greater than 5.6 Å. Thus far, as the H atoms of the *cyclo*-propyl rings are concerned, the shortest intermolecular H⋯H contacts are H9⋯H5 (2.42 Å), H10a⋯H11a (2.56 Å), H10b⋯H10a (2.60 Å), H11a⋯H10a (2.56 Å), and H11b⋯H10a (2.37 Å). Only the last of these is slightly shorter than the expected van der Waals' radius sum of 2.40 Å for two H atoms; thus, we may conclude that van der Waals (dispersion) forces are most important in determining the packing. This is further quantified by the Hirshfeld surface analysis described below.

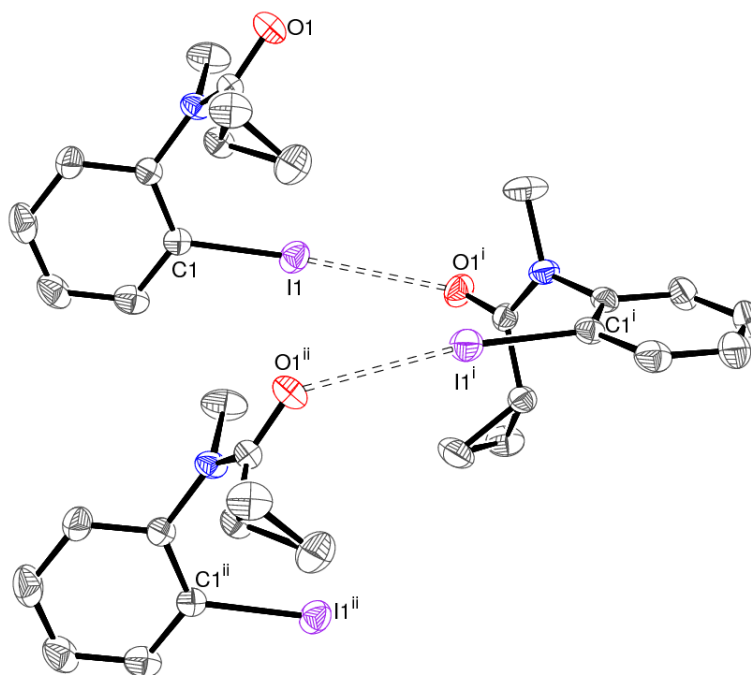


Figure 4. Fragment of an [010] chain of molecules in **1** linked by C—I⋯O halogen bonds (double-dashed lines), with H atoms omitted for clarity. Symmetry codes: (i) $1-x, y-\frac{1}{2}, -z$, (ii) $x, y+1, z$.

3.2. Structure of $C_{15}H_{14}INO$ (**2**)

The structure of **2** (Figure 5), which crystallizes in the orthorhombic space group $P2_12_12_1$, reveals the presence of two molecules in the asymmetric unit, viz., **2A** (containing C1) and **2B** (containing C16). The *cyclo*-heptyl ring of molecule **2B** is disordered over two orientations in a 0.60 (4):0.40 (4) ratio. In **2A**, the dihedral angle between the C1–C6 benzene ring and the C7/N1/C8/O2 methyl-amide group is 89.2 (3)°, and the equivalent angle between the C16–C21 and C22/N2/C23/O2 groupings in **2B** is 89.0 (3)°. As in **1**, both methyl-amide groupings adopt *syn* conformations ($C7-N1-C8-O1 = 0.8$ (11)° for the **2A** molecule and $C22-N2-C23-O2 = 2.9$ (10)° for the **2B** molecule). The dihedral angles between the methyl-amide groupings and *cyclo*-heptyl rings (all atoms, major conformation for the disordered ring) are 79.8 (3)° for **2A** and 81.2 (5)° for **2B**, and the corresponding angles between the benzene and *cyclo*-heptyl rings are 85.4 (3) and 64.2 (4)°, respectively. As in **1**, the H atoms of the methine groups of the *cyclo*-heptyl rings in both molecules of **2** appear to be well-aligned to participate in a translocation reaction with $H9\cdots C1 = 2.79$ Å and $C9-H9\cdots C1 = 130^\circ$ for **2A**, and $H24\cdots C16 = 2.80$ Å and $C24-H24\cdots C16 = 129^\circ$ for **2B**. The conformation of the *cyclo*-heptyl ring in molecule **2A** is well-described as a chair, with C10/C11/C14/C15 approximately coplanar (r.m.s. deviation = 0.045 Å), and C9, C12, and C13 displaced by -0.686 (12), 1.188 (15), and 0.954 (18) Å, respectively: the C11–C12–C13–C14 torsion angle is 27 (1)°. The interpretation of the geometry of the **2B** ring is complicated by disorder, but the major conformation approximates to at least a chair with

C24/C25/C28/C29 roughly coplanar (r.m.s. deviation = 0.124 Å) and C26, C27, and C30 deviating by 0.74 (3), 1.08 (3), and -0.609 (17) Å, respectively.

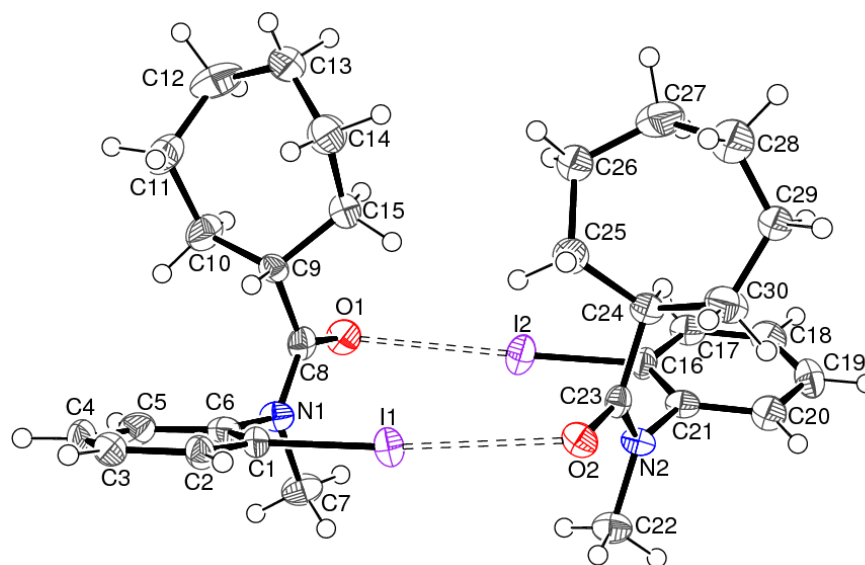


Figure 5. The molecular structure of **2** showing 50% displacement ellipsoids for the non-hydrogen atoms and the short I \cdots O contacts indicated by double-dashed lines. Only one orientation of the disordered *cyclo*-heptyl ring of molecule **2B** is shown.

In the crystal of **2**, the asymmetric molecules associate into dimers with approximate local C_2 symmetry, linked by pairs of C—I \cdots O interactions with a slight asymmetry between the I \cdots O separations (3.024 (4) and 3.057 (4) Å) and C—I \cdots O angles (171.71 (17) and 175.98 (16) $^\circ$), which could possibly be ascribed to packing effects (see Table 1 for the full geometrical details). Otherwise, no directional intermolecular interactions beyond normal van der Waals contacts could be identified: the shortest contact between hydrogen atoms is H15 \cdots H28b at 2.38 Å.

3.3. Hirshfeld Surface Analyses

In order to further quantify the intermolecular interactions in these crystals, their Hirshfeld surfaces were generated using *CrystalExplorer* [15] following the methodology described by Tan et al. [16]. The Hirshfeld surface of **1** (Figure 6) shows intense red spots in the vicinity of atoms O1 and I1, which clearly correlate the halogen bond described above. Otherwise, the surface is blue, indicating contacts at the expected van der Waals' distance or greater.

The percentage contributions of the different types of interactions identified in two-dimensional fingerprint plots [17] are listed in Table 2.

Table 2. Contributions of the different intermolecular interactions to the Hirshfeld surfaces (percentages).

Contact Type	1	2A	2B *
H \cdots H	58.6	67.5	67.2
H \cdots O/O \cdots H	15.3	6.5	5.5
H \cdots I/I \cdots H	14.7	12.0	12.3
H \cdots C/C \cdots H	6.8	10.3	11.5
O \cdots I/I \cdots O	4.1	2.6	2.6
Others	0.5	1.1	0.9

* Major conformation.

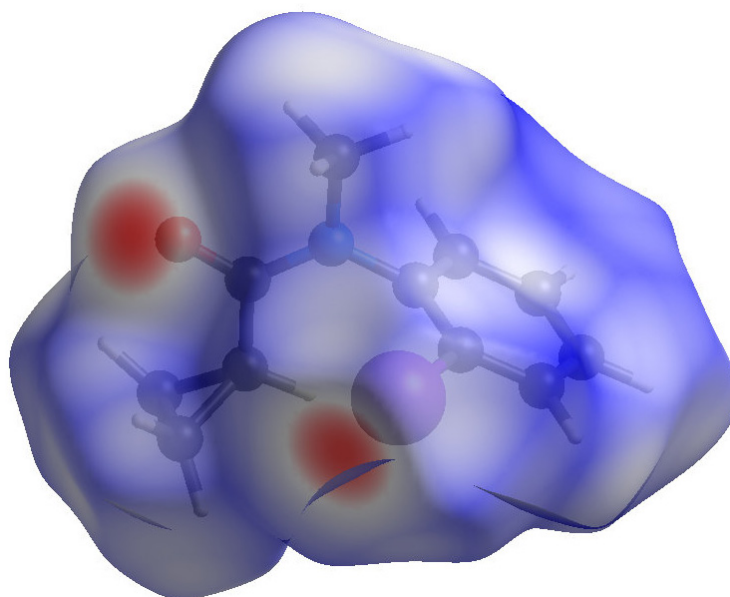


Figure 6. The Hirshfeld surface of **1** plotted as d_{norm} between -0.29 and 1.22 (arbitrary units).

These data indicate that the H···H contacts are the most important in both structures, with a significantly higher percentage for **2** than **1**, although this is not consistent with the atom percentages of hydrogen in the structures (44% H in **2** versus 46% H in **1**). The O···H/H···O contacts in **1** contribute almost three times as much to the surface as in **2**, whereas the H···C/C···H contacts in **2** are almost double those in **1**. Despite their presumed importance in establishing the packing, the I···O interactions only contribute a very modest percentage to the surfaces. The fingerprint plot for the I···O contacts for **1** (Figure 7) shows distinctive ‘crescent’ shapes with the tips at $d_i + d_e \approx 3.0 \text{ \AA}$, obviously corresponding to the I···O separation established in the crystal structure.

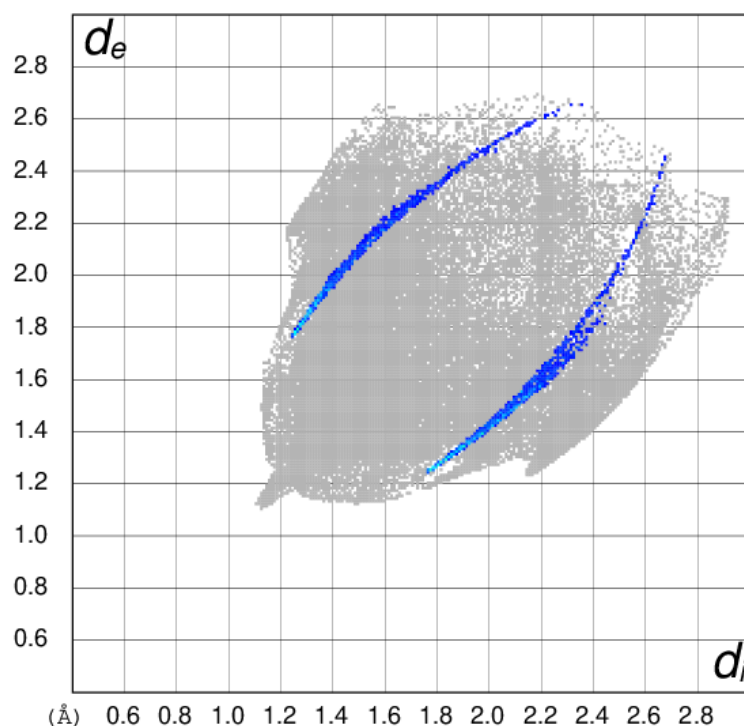


Figure 7. Two-dimensional fingerprint plot of d_e versus d_i for **1**, with the regions corresponding to the I···O contacts highlighted in blue.

3.4. Comparison with Related Structures

The *syn* orientation of the methyl-amide group is common to all three molecules (**1**, **2A**, and **2B**) and is by far the most common geometry for this grouping: a survey of the Cambridge Structural Database [18] yielded the scatterplot shown in Figure 8, which compares the C1—C6—N1—C8 (φ) and C7—N1—C8—O1 (ξ) torsion angles (using the atom numbering in this paper) for some 120 different structures. The methyl-amide torsion angles are heavily clustered in the range $-10^\circ < \xi < 10^\circ$, with one or two outliers with $|\xi| > 160^\circ$ (i.e., corresponding to an *anti*-conformation for the C—N—C—O grouping), which might be attributable to severe steric strain. The φ angle (equivalent to the torsion angle between the benzene ring and the methyl-amide group) shows clustering around $\varphi = \pm 90^\circ$, i.e., a near-perpendicular arrangement in all cases.

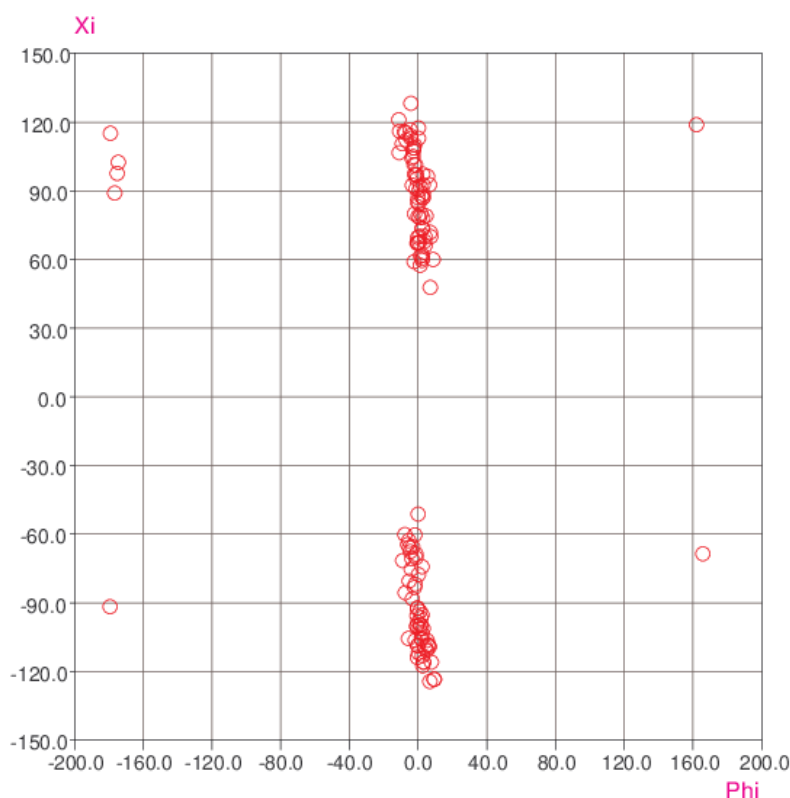


Figure 8. Scatterplot of the ξ (ξ) and φ (φ) torsion angles (see the text).

4. Conclusions

We have prepared and structurally characterized the related compounds $C_{11}H_{12}INO$ (**1**) and $C_{15}H_{14}INO$ (**2**) as possible precursors for radical cyclization translocation reactions: the donor H atom and the pre-radical C—I bond appeared to be well-aligned in the solid state for this to occur. The crystals of both compounds featured short C—I \cdots O halogen bonds, which generated chains in **1** and dimers in **2**. A survey of the Cambridge Structural Database showed that almost all methyl-amide groups adopted a *syn* confirmation, and when this grouping was bonded to a benzene ring, the moieties were orientated approximately normal to each other. The Hirshfeld surfaces indicated that the I \cdots O contacts made a modest percentage contribution.

Author Contributions: Conceptualization, J.M.D.S.; synthesis and spectroscopy, A.I.; crystallography, W.T.A.H.; writing, W.T.A.H. All authors have read and agreed to the published version of the manuscript.

Funding: This research received no external funding.

Institutional Review Board Statement: Not applicable.

Informed Consent Statement: Not applicable.

Data Availability Statement: CCDC 2254542 and 2254543 contain the supplementary crystallographic data for this paper. These data can be obtained free of charge via: www.ccdc.cam.ac.uk/data_request/cif (accessed on 2 May 2023), by e-mailing data_request@ccdc.cam.ac.uk, or by contacting The Cambridge Crystallographic Data Centre, 12, Union Road, Cambridge CB2 1EZ, UK; fax: +44-1223336033.

Acknowledgments: We thank the EPSRC National Crystallography Service (University of Southampton, England) for the X-ray data collection for 2.

Conflicts of Interest: The authors declare no conflict of interest.

References

1. Renauld, P.; Sibi, M.P. *Radicals in Organic Synthesis*; Wiley-VCH: Weinheim, Germany, 2002; Volume 1–2.
2. Takeda, Y.; Nakabayashi, T.; Shirai, A.; Fukumoto, D.; Kiguchi, T.; Naito, T. A formal synthesis of martinelline via a combination of two types of radical reactions. *Tetrahedron Lett.* **2004**, *45*, 3481–3484. [[CrossRef](#)]
3. Chakraborty, T.K.; Chattopadhyay, A.K.; Ghosh, S. Total synthesis of (+)-blastmycinone and formal synthesis of (+)-antimycin A(3b). *Tetrahedron Lett.* **2007**, *48*, 1139–1142. [[CrossRef](#)]
4. Montevicchi, P.C.; Navacchia, M.L. Rearrangements and cyclizations in vinyl radicals. Unusual example of 1,4-radical translocation. *Tetrahedron Lett.* **1996**, *36*, 6583–6586. [[CrossRef](#)]
5. Van Dort, P.C.; Fuchs, P.L. Free radical self-immolative 1,2-elimination and reductive desulfonylation of aryl sulfones promoted by intramolecular reactions with ortho-attached carbon-centered radicals. *J. Org. Chem.* **1997**, *62*, 7142–7147. [[CrossRef](#)] [[PubMed](#)]
6. Curran, D.P.; Shen, W. Radical translocation reactions of vinyl radicals—substituent effects on 1,5-hydrogen transfer reactions. *J. Am. Chem. Soc.* **1993**, *115*, 6051–6059. [[CrossRef](#)]
7. Jones, K.; Storey, J.M.D. Aryl radical cyclizations involving an amide group in the linking chain. *J. Chem. Soc. Chem. Commun.* **1992**, 1766–1767. [[CrossRef](#)]
8. Dorigo, A.E.; Houk, K.N. Transition structures for intramolecular hydrogen-atom transfers—The energetic advantage of 7-membered over 6-membered transition structures. *J. Am. Chem. Soc.* **1987**, *109*, 2195–2197. [[CrossRef](#)]
9. Penn, R.E.; Boggs, J.E. Substituent-induced asymmetry of the cyclopropane ring. *J. Chem. Soc. Chem. Commun.* **1972**, 666–667. [[CrossRef](#)]
10. Desiraju, G.R.; Shing Ho, P.; Kloo, L.; Legon, A.C.; Marquardt, R.; Metrangolo, P.; Politzer, P.; Resnati, G.; Rissanen, K. Definition of the halogen bond. *Pure Appl. Chem.* **2013**, *85*, 1711–1713. [[CrossRef](#)]
11. Bondi, A. van der Waals' volumes and radii. *J. Phys. Chem.* **1964**, *68*, 441–451. [[CrossRef](#)]
12. Mallada, B.; Gallardo, A.; Lamanec, M.; De La Torre, B.; Spirko, V.; Hobza, P.; Jelinek, P. Real-space imaging of anisotropic charge of σ -hole by means of Kelvin probe force microscopy. *Science* **2021**, *374*, 863–867. [[CrossRef](#)] [[PubMed](#)]
13. Metrangolo, P.; Neukirch, H.; Pilati, T.; Resnati, G. Halogen bonding based recognition processes: a world parallel to hydrogen bonding. *Acc. Chem. Res.* **2005**, *38*, 386–395. [[CrossRef](#)] [[PubMed](#)]
14. Etter, M.C. Encoding and decoding hydrogen-bond patterns of organic-compounds. *Acc. Chem. Res.* **1990**, *23*, 120–126. [[CrossRef](#)]
15. Turner, M.J.; Mckinnon, J.J.; Wolff, S.K.; Grimwood, D.J.; Spackman, P.R.; Jayatilaka, D.; Spackman, M.A. *Crystal Explorer 17*; The University of Western Australia: Crawley, WA, Australia, 2017.
16. Tan, S.L.; Jotani, M.M.; Tiekink, E.R.T. Utilizing Hirshfeld surface calculations, non-covalent interaction (NCI) plots and the calculation of interaction energies in the analysis of molecular packing. *Acta Cryst.* **2019**, *E75*, 308–318. [[CrossRef](#)] [[PubMed](#)]
17. Spackman, M.A.; Mckinnon, J.J. Fingerprinting intermolecular interactions in molecular crystals. *CrystEngComm* **2002**, *4*, 378–392. [[CrossRef](#)]
18. Allen, F.H.; Motherwell, W.D.S. Applications of the Cambridge Structural Database in organic chemistry and crystal chemistry. *Acta Cryst.* **2002**, *B58*, 407–422. [[CrossRef](#)] [[PubMed](#)]

Disclaimer/Publisher's Note: The statements, opinions and data contained in all publications are solely those of the individual author(s) and contributor(s) and not of MDPI and/or the editor(s). MDPI and/or the editor(s) disclaim responsibility for any injury to people or property resulting from any ideas, methods, instructions or products referred to in the content.